Glancing Angle Deposited CdTe: Optical Properties and Structure

Dipendra Adhikari, Prakash Koirala, Maxwell M. Junda, Robert W. Collins, and Nikolas J. Podraza

Wright Center for Photovoltaics Innovation and Commercialization & Department of Physics and Astronomy, University of Toledo, Toledo, OH, 43606, USA

***Abstract* — Optical and microstructural properties of as-deposited CdTe films deposited on soda lime glass by magnetron sputtering at various source flux angles have been investigated using GIXRD, SEM, unpolarized transmittance / reflectance, and spectroscopic ellipsometry. Influence of deposition angle on resultant crystalline grain size and orientation are tracked for these films. All CdTe films studied are found to have cubic crystal structure and (111) preferential grain orientation. Films deposited at 0° and 45° are almost entirely (111) oriented, whereas films deposited at higher angles exhibit a wider variety of competing grain orientations, suggesting that deposition angle can be used as an effective parameter towards controlling grain orientation. With increasing numbers of grain orientations, grain size is found to decrease. *Ex-situ* spectroscopic ellipsometry is used to obtain the structural and optical properties. Stress induced in the film is calculated based on shifts of critical point energies.**

***Index Terms* — glancing angle deposition, ellipsometry, complex dielectric function.**

I. Introduction

Cadmium Telluride (CdTe) is a II-IV group semiconductor that is successfully used as an absorber layer in thin film photovoltaics (PV) mainly as a result of its high optical absorption of >10^4 cm^{-1} in visible range, a direct band gap around 1.5 eV, and sufficiently high electronic quality. CdTe absorbers can be deposited by a variety of deposition techniques including sputtering, spray pyrolysis, electrodeposition, close-space sublimation (CSS), etc. The microstructure of CdTe films depends on various deposition parameters and plays an important role in PV device performance. Using glancing angle deposition, the microstructure of CdTe films can potentially be engineered, resulting in the ability to tune opto-electronic properties for PV optimization. This work involves study of such CdTe films deposited via glancing angle radio frequency (RF) sputtering with material flux at various angles relative to the substrate normal. In particular, the influence of deposition angle on the microstructural and optical properties of sputtered CdTe film are studied. Resulting properties of the films are measured using grazing incidence x-ray diffraction (GIXRD), scanning electron microscopy (SEM), and spectroscopic ellipsometry (SE). The deposition angle is found to be related to resultant crystallite grain size and orientation and is also found to influence film optical properties.

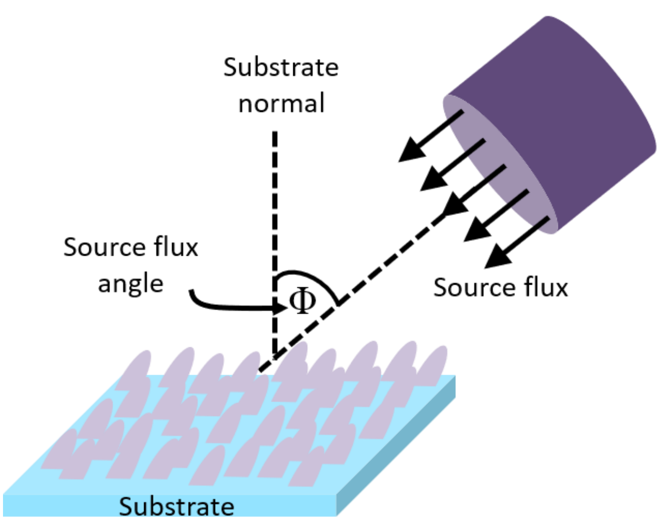

Fig. 1. Schematic of glancing angle deposition.

Polycrystalline CdTe absorbers for solar cells consist of crystalline grains/grain boundary regions and photovoltaic device performance depends upon both CdTe grain and grain boundaries characteristics. Previous studies show that the depleted grain boundaries are beneficial to CdTe solar cell performance by helping to separate carriers, suppress recombination, and improve carrier collection [1][2]. Glancing angle deposition (GLAD) produces films with varying preferential grain orientations and grain boundary configurations. Here the source flux angle controls grain orientation of CdTe and grain boundary configuration. Atomic scale self-shadowing can result in different film microstructures and porosity. Here the source flux angle controls grain orientation of CdTe and grain boundary configuration. The dependence of grain size, grain orientation, film stress, and optical properties on source flux angle are identified.

II. Experimental Details

The CdTe films are RF magnetron sputtered onto soda lime glass substrates mounted at 0°, 45°, 55°, 65°, 75°, and 85° source flux angles (Φ) relative to the substrate normal as illustrated in Fig. 1. The glass substrates were cleaned via ultrasonication and dried with N_2 before deposition. During deposition, a CdTe target of 99.999% purity was sputtered in an Ar ambient of 10 mTorr with an RF power of 200 W and a substrate temperature of 250°C. X-ray diffraction (XRD) data were collected with a Raguku Ultima III diffractometer using Cu-Kα radiation (λ = 1.543Å) at 1° glancing angle. Ellipsometric spectra were collected at 70° incidence angle covering 0.74 – 5.88 eV spectral range using a single rotating compensator multichannel ellipsometer (M-2000, J. A. Woollam Co.).

III. Results and Discussion

Fig. 2 compares the GIXRD patterns of the CdTe films deposited at various incident flux angles and shows diffraction peaks corresponding to (111), (220), (311), (400), and (331) plane orientations of cubic zinc-blende crystal structure with *F-43m* space group. All CdTe films studied are found to have (111) preferential grain orientation. Films deposited at 0° and 45° are almost entirely (111) oriented, whereas films deposited at higher angles exhibit a wider variety of competing grain orientations, indicating that deposition angle can be used as an effective parameter towards controlling grain orientation. The film deposited at 65° glancing angle exhibits the widest distribution of grain orientations. As a simple measure of the extent to which deposition angle promotes varied grain orientations, the ratio of peak intensities corresponding to (220) and (111) planes are plotted in Fig. 3.

The average grain size shown in Fig. 4 is calculated using Scherrer's formula,

$$d = k\lambda/\beta cos\theta \qquad (1)$$

where the shape factor k = 0.9, λ is the x-ray wavelength (1.54059 Å for Cu_{α}), β is the diffraction peak full width at half maximum, and θ is the diffraction angle. Fig. 5 presents the variation in peak intensity ratio, $I_{(220)}/I_{(111)}$, with grain size. Comparing Figs. 3, 4, and 5, the increased distribution of grain orientations is related to decreases in average grain size. This is most evident for the film deposited at 65° where, compared to other samples, a significantly increased portion of (220) oriented grains is accompanied by the smallest overall grain size. A likely explanation for this behavior is that increased

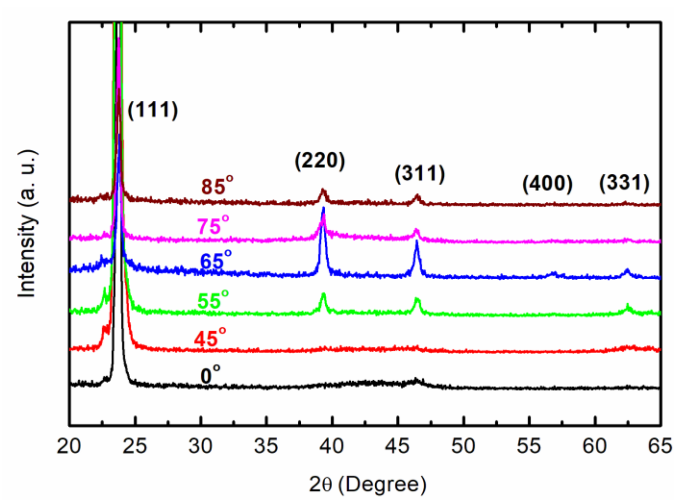

Fig. 2. Grazing incidence x-ray diffraction (GIXRD) patterns of CdTe films deposited at different glancing angles.

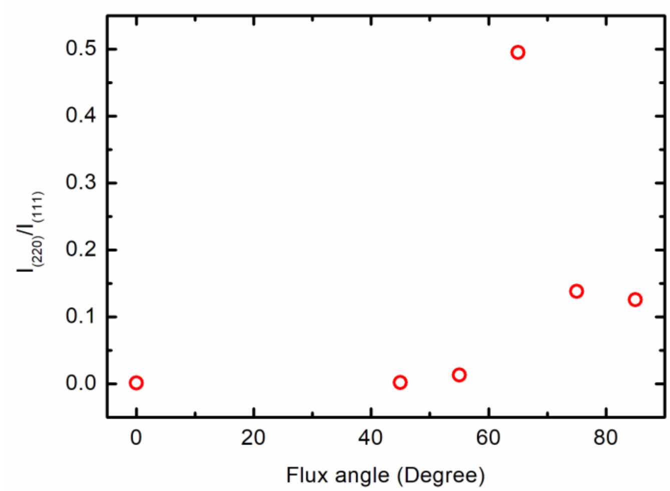

Fig. 3. Ratio of (220) to (111) peak intensities versus incident flux angle.

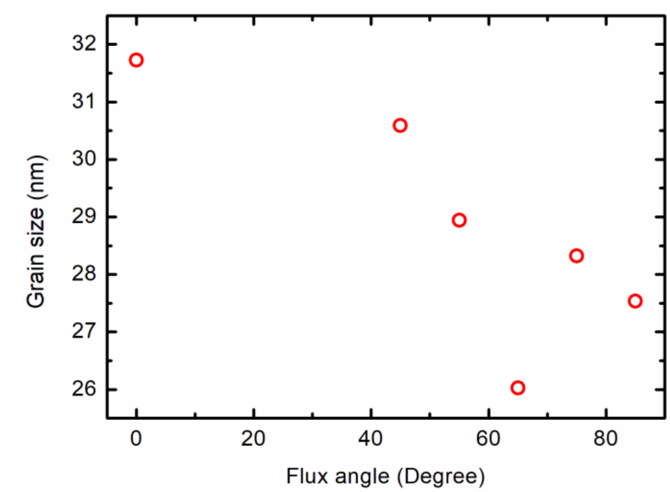

Fig. 4. Grain size as a function of incident flux angle.

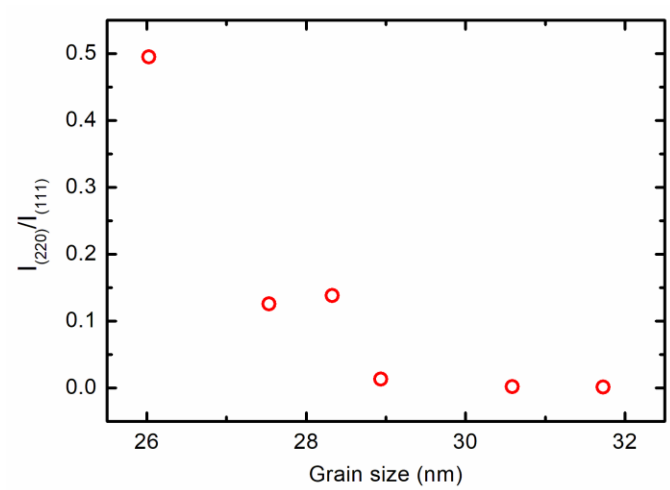

Fig. 5. Correlation of (220) to (111) peak intensity ($I_{(220)}/I_{(111)}$) with grain size of CdTe films deposited at different glancing angles.

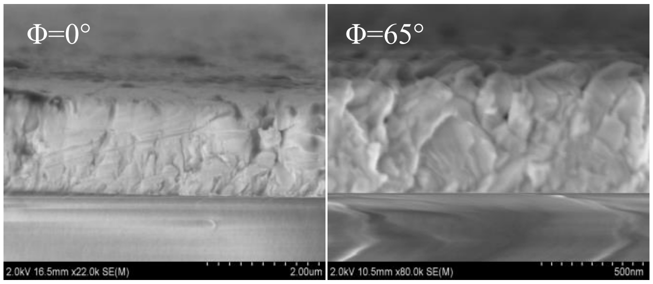

Fig. 6. Cross-section scanning electron microscopy (SEM) images of CdTe films deposited at Φ = 0° and 65°.

competition between the growth of multiple grain orientations suppresses any single orientation's ability to grow unimpeded to large grain sizes. The cross-sectional SEM images obtained for films with Φ = 0° and 65° are depicted in Fig. 6 and show dense polycrystalline CdTe films.

A structural-optical model is applied to SE measurements to obtain the complex dielectric function ($\varepsilon = \varepsilon_1 + i\varepsilon_2$) spectra of all CdTe films. Structurally, the model consists of a glass substrate / bulk CdTe film / surface roughness. The optical responses of the surface roughness and are described by a Bruggeman effective medium approximation consisting of two material components, material and void [3]. Bulk-CdTe in ε was parameterized with a combination of oscillators describing electronic transitions assuming critical point parabolic bands (CPPB) [4][5] and a Tauc-Lorentz (TL) oscillator [6]. Fig. 7 shows spectra in ε for bulk CdTe films deposited at different source flux angles during sputtering with optical contrast observed. Four critical point features represented as E_o, E_1, $E_1+\Delta_1$, and E_2 with resonance energies near 1.491, 3.310, 3.894, and 5.160 eV corresponding to single crystal CdTe have been observed for all samples. Alternatively, the index of refraction (n) and the absorption coefficient (α) are calculated using

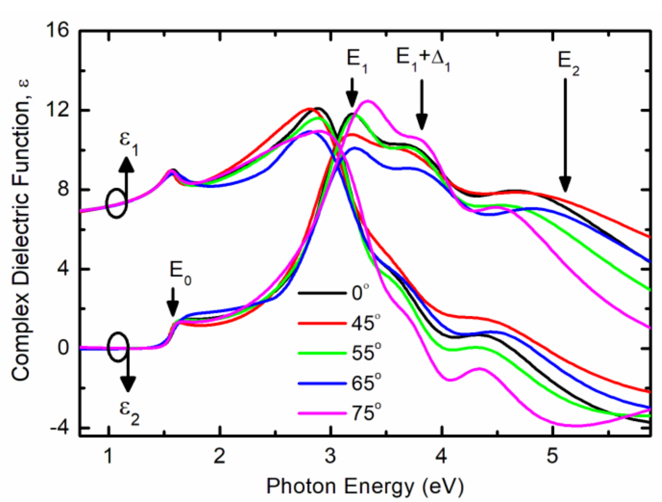

Fig. 7. Complex dielectric function ($\varepsilon = \varepsilon_1 + i\varepsilon_2$) spectra for CdTe films deposited at different incident source flux angle. The arrow shows four critical points observed.

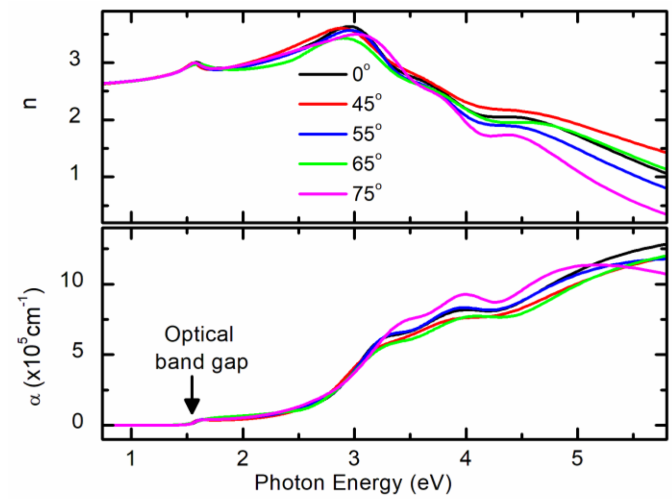

Fig. 8. Index of refraction (n) and absorption coefficient (α) for CdTe deposited at different incident source flux angles.

spectra in ε, obtained from ellipsometry with the expressions,

$$n = \frac{1}{\sqrt{2}}\left\{\sqrt{(\varepsilon_1{}^2 + \varepsilon_2{}^2)} + \varepsilon_1\right\}^{1/2} \quad (2)$$

$$\alpha = \frac{4\pi}{\sqrt{2}\lambda}\left\{\sqrt{(\varepsilon_1{}^2 + \varepsilon_2{}^2)} - \varepsilon_1\right\}^{1/2} \quad (3)$$

Fig. 8 shows the optical response of CdTe films deposited at different glancing angles and exhibits similar low photon energy index of refraction (n) indicating consistent optical density and non-varying band gap energies. However, the higher energy critical points (CPs) vary somewhat in amplitude

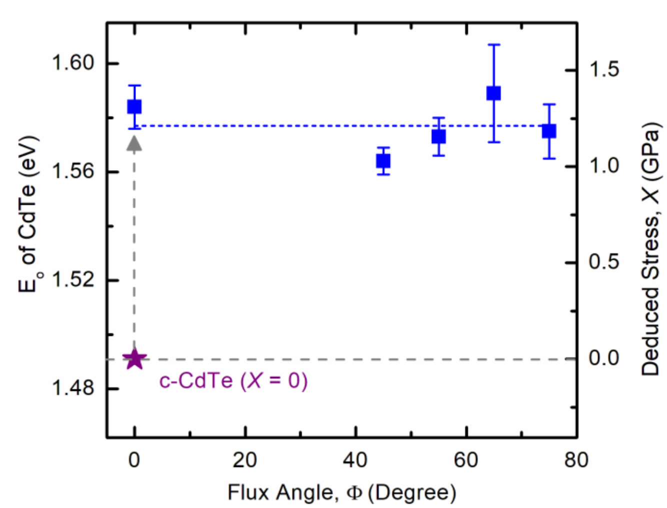

Fig. 9. The E_o critical point energies (left scale) and deduced in-plane compressive stress (right scale) for CdTe films (squares) as a function of incident source flux angle.

indicating subtle differences in above gap transition strengths possibly stemming from different grain / grain boundary configurations.

Shifts in CP transition energies from those for single crystal c-CdTe are used as a probe of stress (*X*) in polycrystalline CdTe thin films. Compressive in-plane stress in as-deposited CdTe films prepared at different glancing angles are calculated using linear stress coefficient, $C_X(E_o) = 0.071$ eV/GPa for E_o [7]. Fig. 9 presents the in-plane stress in an as-deposited CdTe films as a function of glancing angle Φ. We have observed that the source flux angle does not substantially alter film stress in as-deposited CdTe films.

VI. Conclusions

RF sputtered glancing angle deposited CdTe films exhibit cubic zinc blende crystal structure with (111) preferred orientation at lower source flux angles and more random orientations at higher angles. Comparable film density, band gap energy, and stress are observed for all samples deposited at different source flux angles. Only grain orientation and grain boundary configuration are manipulated by source flux angle. GLAD of CdTe provides a possible tool for understanding how initial grain boundary configuration in polycrystalline thin films impact final device performance and the effectiveness of post-deposition processes, such as $CdCl_2$ treatment, in altering film structure and electronic quality.

Acknowledgement

This work was supported by National Science Foundation (NSF), Grant No. 1711534.

References

[1] C. Li, Y. Wu, J. Poplawsky, T. J. Pennycook, N. Paudel, W. Yin, S. J. Haigh, M. P. Oxley, A. R. Lupini, M. Al-Jassim, S. J. Pennycook, and Y. Yan, Grain-boundary-enhanced carrier collection in CdTe solar cells, *Phys. Rev. Lett.,* vol. 112, p. 156103, 2014.

[2] I. Visoly-Fisher, S.R. Cohen, A. Ruzin, D. Cahen, How polycrystalline devices can outperform single-crystal ones: thin film CdTe/CdS solar cells, *Adv. Mater.,* vol. 16, pp. 879–883, 2004.

[3] H. Fujiwara, J. Koh, P. Rovira, R. Collins, Assessment of effective-medium theories in the analysis of nucleation and microscopic surface roughness evolution for semiconductor thin films. *Phys. Rev. B,* vol. 61, pp. 10832-10844, 2000.

[4] D. E. Aspnes, *Handbook of Semiconductors*; Vol. 2, edited by M. Balkanski; North-Holland: Amsterdam, The Netherlands*,* 1980.

[5] R. W. Collins and A. S. Ferlauto, *Handbook of Ellipsometry*, edited by H. G. Tompkins and E. A. Irene (William Andrew publishing, Norwich), 2005.

[6] G. E. Jellison, Jr. and F. A. Modine, Parameterization of the optical functions of amorphous materials in the interband region, *Appl. Phys. Lett.* vol. 69, pp. 371-373, 1996.

[7] J. Li, J. Chen, and R. W. Collins, Optical transition energies as a probe of stress in polycrystalline CdTe thin films, *Appl. Phys. Lett.,* vol. 99, p. 061905, 2011.